Clinical Cancer Research

Telomerase Activation and ATRX Mutations Are Independent Risk Factors for Metastatic Pheochromocytoma and Paraganglioma

Sylvie Job[1], Irena Draskovic[2,3], Nelly Burnichon[4,5,6], Alexandre Buffet[4,5], Jérôme Cros[7], Charles Lépine[5,6], Annabelle Venisse[6], Estelle Robidel[4,5], Virginie Verkarre[8], Tchao Meatchi[8], Mathilde Sibony[9,10], Laurence Amar[4,5,11], Jérôme Bertherat[9,12], Aurélien de Reyniès[1], Arturo Londoño-Vallejo[2,3], Judith Favier[4,5], Luis Jaime Castro-Vega[4,5], and Anne-Paule Gimenez-Roqueplo[4,5,6,1,2]

Abstract

Purpose: Pheochromocytomas and paragangliomas (PPGLs) are rare neuroendocrine tumors. Whereas most PPGLs are benign, up to 20% may become metastatic with *SDHB*- and *FH*-mutated tumors showing the higher risk. We aimed at determining the contribution of immortalization mechanisms to metastatic progression.

Experimental Design: Immortalization mechanisms were investigated in 200 tumors. To identify telomerase (+) tumors, we analyzed genomic alterations leading to transcriptional activation of *TERT* comprising promoter mutations, hypermethylation and gain copy number. To identify tumors that activated the alternative lengthening of telomere (ALT) mechanism, we combined analyses of telomere length by slot blot, telomere heterogeneity by telomere FISH, and *ATRX* mutations by next-generation sequencing. Univariate/multivariate and metastasis-free survival (MFS) and overall survival (OS) analyses were carried out for assessment of risk factors and clinical outcomes.

Results: Only 37 of 200 (18.5%) tumors achieved immortalization. Telomerase activation occurred in 12 metastatic tumors and was prevalent in *SDHB*-mutated paragangliomas ($P = 2.42e{-}09$). ALT features were present in 25 tumors, mostly pheochromocytomas, regardless of metastatic status or molecular group ($P = 0.169$), yet *ATRX* mutations were found preferentially in *SDHB*/*FH*-mutated metastatic tumors ($P = 0.0014$). Telomerase activation and *ATRX* mutations were independent factors of poor prognosis: MFS (hazard ratio, 48.2 and 33.1; $P = 6.50E{-}07$ and $1.90E{-}07$, respectively); OS (hazard ratio, 97.4 and 44.1; $P = 4.30E{-}03$ and $2.00E{-}03$, respectively) and were associated with worse MFS and OS (log-rank tests $P < 0.0001$).

Conclusions: Assessment of telomerase activation and *ATRX* mutations could be used to identify metastatic PPGLs, particularly in tumors at high risk of progression.

Introduction

Pheochromocytomas and paragangliomas (PPGLs) are neuroendocrine tumors arising from adrenal medulla and paraganglia, respectively. Although the majority of PPGLs never progress, it has been estimated that up to 20% can develop overt metastases (1).

Metastatic PPGLs represent a major clinical challenge due to the limitations in accurate diagnosis and effective treatments. Indeed, reliable tumor biomarkers are still lacking to distinguish, at the time of diagnosis, tumors that will remain benign from those that will progress to metastasis. Consequently, the diagnosis of metastasis remains the only definitive criterion to define malignant PPGLs according to the most recent World Health Organization (WHO) classification (2) and a life-long follow-up is recommended for every patient presenting with PPGLs, despite the fact that most are usually cured after surgery.

PPGLs are characterized by a remarkable genetic determinism with up to 40% of cases explained by germline mutations in 14 susceptibility genes comprising *SDHA*, *SDHB*, *SDHC*, *SDHD*,

[1]Programme Cartes d'Identité des Tumeurs, Ligue Nationale Contre Le Cancer, Paris, France. [2]CNRS, UMR3244, Institut Curie, PSL Research University, Paris, France. [3]Sorbonne Universités, UPMC, Univ Paris 06, Paris, France. [4]INSERM, UMR970, Paris-Cardiovascular Research Center, Equipe Labellisée par la Ligue contre le Cancer, Paris, France. [5]Université Paris Descartes, Sorbonne Paris Cité, Faculté de Médecine, Paris, France. [6]Assistance Publique-Hôpitaux de Paris, Hôpital Européen Georges Pompidou, Department of Genetics, Paris, France. [7]INSERM, UMR1149, Hôpital Beaujon, Department of Pathology, Clichy, France. [8]Assistance Publique-Hôpitaux de Paris, Hôpital Européen Georges Pompidou, Department of Pathology, Paris, France. [9]INSERM, U1016, Institut Cochin, Paris, France. 10 CNRS UMR8104, Paris, France. [10]Assistance Publique Hôpitaux de Paris, Hôpital Cochin, Department of Pathology, Paris, France. [11]Assistance Publique-Hôpitaux de Paris, Hôpital Européen Georges Pompidou, Hypertension Unit, Paris, France. [12]Rare Adrenal Cancer Network COMETE, Paris, France.

Note: Supplementary data for this article are available at Clinical Cancer Research Online (http://clincancerres.aacrjournals.org/).

S. Job, I. Draskovic, and N. Burnichon contributed equally to the article.

J. Favier, L.J. Castro-Vega, and A.-P. Gimenez-Roqueplo jointly directed the article.

Corresponding Author: Luis Jaime Castro-Vega, INSERM, 56 rue Leblanc, 75015 Paris, France. Phone: 15-398-8045; E-mail: luis-jaime.castro-vega@inserm.fr

doi: 10.1158/1078-0432.CCR-18-0139

Translational Relevance

Pheochromocytomas and paragangliomas (PPGLs) are tumors of neural crest origin with *SDHB*/*FH*-mutated carriers showing a high risk of metastatic progression. At present, it is not possible to distinguish benign from metastatic PPGLs based on histopathologic features. A better understanding of the underlying mechanisms of metastatic PPGLs is critical for the successful identification of risk factors able to predict PPGL behavior. Here, we identified genomic alterations leading to telomerase activation (*TERT* promoter mutation/hypermethylation and gain copy number) and *ATRX* mutations in most metastatic PPGLs, particularly *SDHB*/*FH*-mutated tumors. Remarkably, these immortalization-related mechanisms were independent factors of poor prognosis associated with shorter metastasis-free and overall survival. Therefore, assessment of telomerase activation mechanisms and screening of *ATRX* mutations could be used in the clinical routine to discriminate metastatic from nonmetastatic PPGLs at high risk of progression.

SDHAF2 (collectively referred to as *SDHx*), *FH*, *MDH2*, *SLC25A11* (3), *EPAS1*, *VHL*, *NF1*, *RET*, *TMEM127*, and *MAX* (4, 5). Importantly, *SDHB*/*FH* mutations are associated with high risk of metastatic progression and poor prognosis (6–8), with about half of the mutation carriers presenting synchronous or metachronous metastases. Clinical characteristics such as primary tumor size and extra-adrenal location have been suggested as risk factors as well (9).

Genomics studies revealed that PPGL tumorigenesis is mainly driven by germline or somatic mutations in susceptibility genes, but they failed to identify recurrent genetic alterations linked to metastatic progression (10). Transcriptomic unsupervised classification established 3 main clusters: Krebs cycle cluster C1A, comprising tumors at high risk of metastatic progression (*SDHx*, *FH*-, *MDH2*- and *SLC25A11*-mutated), the pseudohypoxic cluster C1B mostly specific of *VHL*-mutated tumors, and the kinase signaling cluster C2 comprising *NF1*-, *RET*-, *HRAS*-, *TMEM127*-, *MAX*-mutated tumors (11).

We hypothesized that immortalization in primary PPGLs could be an important risk factor for progression toward metastasis. Immortalization is achieved by reactivation of telomerase in about 85% of human carcinomas (12) or by a recombination-based alternative lengthening of telomeres (ALT) pathway mainly in sarcomas and tumors arising from endocrine and neural tissues (13). The specific contribution of these immortalization mechanisms to PPGL progression remains undetermined.

Telomerase activation can be assessed by evaluation of *TERT* expression (14). However, given the possible lymphocytic infiltration in tumors, expression of *TERT* alone should be taken with caution and additional efforts are required to analyze underlying mechanisms such as *TERT* promoter mutations (15), hypermethylation (16), amplifications (17), and genomic rearrangements (15). On the other hand, the genetic basis of ALT tumors remains poorly defined, although mutations in *ATRX* have been reported to be associated with this phenotype (18).

Early studies reported telomerase overexpression in malignant pheochromocytomas (19–23), whereas *TERT* promoter mutations (24, 25) and hypermethylation (26) were recently found in a few *SDHx*-deficient paragangliomas. The phenotypic assignment of ALT based on telomeric analysis of histological preparations remains limited to 2 discrepant studies reporting a prevalence of 4% (27) and 27% (28) of 75 and 22 PPGLs, respectively. Also, mutations in *ATRX*, were reported to occur in 12.6% of PPGLs, some associated with ALT and aggressive features (28). However, fewer mutations were detected in exome sequencing studies (29–33). So far, no systematic study has concomitantly analyzed both telomere maintenance mechanisms, which is necessary to determine the actual prevalence of immortalization and its relative contribution for metastatic progression.

Here, we performed a comprehensive analysis of immortalization in a well-characterized series of 200 PPGLs by combining previous multiomics data (29) with experimental validations (Supplementary Fig. S1). We aimed at identifying telomerase (+) and ALT (+) tumors while ascertaining their association with underlying mechanisms, genetic status, clinical features and outcomes of affected patients. We provide solid evidence that telomerase activation and *ATRX* mutations help to discriminate metastatic from non-metastatic tumors in high-risk PPGLs, thus suggesting a great clinical potential for diagnostic and eventually for therapeutic purposes.

Materials and Methods

PPGL cohort

Two hundred tumor samples from 190 patients with PPGLs, collected by the French "Cortico et Médullosurrénale: les Tumeurs Endocrines" (COMETE) network (34) were analyzed in this study. The study was conducted in accordance with the Declaration of Helsinki. Ethical approval for the study was obtained from the institutional review board [Comité de Protection des Personnes (CPP) Ile de France III, June 2012]. Written informed consent for the sample collection and subsequent analyses was obtained from all patients. Mutation status (germline or somatic) for the main PPGL susceptibility genes and integrative genomic characterization of the cohort were previously reported (29). For this study, we also identified 7/200 (3.5%) *MAML3* (+) tumors (Supplementary Fig. S2). Primer sequences for amplification of *UBTF–MAML3* fusion transcripts are provided in Supplementary Table S1.

Availability of data

The datasets analyzed during the current study are available in the following repositories: Gene-expression profiling (ArrayExpress entry E-MTAB-733); copy-number alterations (ArrayExpress entry E-MTAB-2817); whole-genome DNA methylation [Gene Expression Omnibus (GEO) entry GSE43298]. Whole-exome sequencing data [European Genome-phenome Archive (entry EGAS00001000933)].

RT-qPCR

Total RNA was purified with the miRNeasy Mini Kit (Qiagen) and cDNAs prepared with the Superscript III Kit (Thermo fisher scientific). Quantitative PCR was performed with iTaq Universal SYBR Green Supermix (Bio-Rad). Primer sequences are provided in Supplementary Table S1. For absolute quantifications of *TERT* variants, cDNA amplicons were purified from agarose gels using NucleoSpin Gel and PCR Clean-up Kit (Macherey-Nagel) to be used as standards. Cycling conditions were as reported (35).

TERT promoter mutations and methylation

Amplicons of 163bp were amplified from tumor DNAs using a set of primers listed in Supplementary Table S1 to target the *TERT* promoter region (chr5:1295151-1295313). PCR was performed with KAPA HiFi HotStart ReadyMix kit (Kapa Biosystems) using 50-ng genomic DNA. Sequencing reactions in both directions were performed in an Applied Biosystems 3730xl DNA Analyzer. *TERT* mutations were confirmed to be present only at the somatic level. For analysis of promoter methylation, pyrosequencing of a region of 36 bp containing 5 CpG sites (chr5:1295586-1295621; GRCh37/hg19) was amplified from sodium bisulfite modified genomic DNA and analyzed as described previously (16). Primers are listed in Supplementary Table S1.

Whole-genome sequencing

To identify *TERT* rearrangements, PCR-free libraries were prepared with NEBNext Ultra II DNA Library Prep Kit following supplier recommendations. Briefly, 300-ng double-strand gDNA from tumor sample CIT_015 were fragmented using a sonication method to obtain 400-bp average sizes. After ligation with paired-end adaptor oligonucleotides (xGen TS-LT Adapter Duplexes from IDT), fragments were purified for direct sequencing. DNA PCR-free library sequencing was performed on an Illumina HiSeq 4000 instrument with a paired-end read length of 150 nucleotides. Base calling and image analysis were performed using Illumina Real Time Analysis (RTA) Pipeline version 1.12.4.2 with default parameters. The Manta software was used for identification of somatic structural variants nearby the *TERT* locus.

Slot blot

50 ng of tumor DNAs were spotted onto Biodyne B nylon membranes in alkaline conditions, hybridized to an oligonucleotide labeled with digoxigenin (DIG) and revealed for the DIG signal following Roche instructions. After stripping, membranes were rehybridized with DIG labeled total genomic DNA from HCA2 primary cells. Quantification of telomeric and genomic signals was performed using the MultiGauge software. Telomeric intensities were normalized with the genomic signal to correct for the differences in ploidy.

APB assays

Detection of ALT-associated PML bodies (APBs) was based on colocalization of a telomeric FISH signal with the PML protein. Tissue sections (4 μm) were steamed with citrate buffer and serially incubated with anti-PML antibody (Chemicon, AB1370) diluted 1/1,000, and goat anti-rabbit alexa 488 antibody diluted 1/100. Slides were post fixed with 3.7% formaldehyde and dehydrated. Hybridization with a Cy3-labeled peptide nucleic acid (PNA) telomere probe (Panagene, F1002) was performed overnight. Slides were imaged with a Nikon 80i epifluorescence microscope. The following ALT characteristics were evaluated: (i) dramatic cell-to-cell telomere length heterogeneity, (ii) the presence of large, ultra-bright nuclear foci of telomere FISH signals in tumor cells, and (iii) colocalization of PML protein with telomeric FISH (APBs).

Screening of *ATRX* mutations

All coding regions of *ATRX* were amplified using the MASTR Plus technology (Agilent technologies) to allow their analysis using Next-Generation Sequencing (NGS). Amplicon libraries from different samples were further processed by bridge amplification followed by sequencing on the MiSeq Instrument using the MiSeq reagent kit v2, 300 cycles. NGS data were analyzed using the SeqNext module v4.3.1 (JSI medical systems) and the PolyDiag pipeline developed by the Paris Descartes bioinformatic platform. Mutations with a ratio >10% were considered relevant. *ATRX* mutations were confirmed to be present only at the somatic level.

Statistical analyses

Associations between molecular and clinical characteristics were evaluated with 2-sided χ^2 or Fisher-exact tests with significance set to $P < 0.05$. Differential analysis was determined using moderated T-tests or ANOVA models for multigroup comparison. In case of significant P values for ANOVA tests, we calculated pairwise comparisons with corrections for multiple testing. Local false discovery rate was used to control for multiple testing using the Benjamini and Hochberg method. The significance of a Pearson coefficient computed on 2 quantitative covariates was estimated by a correlation test based on a Student t distribution of the Pearson correlation coefficient. Univariate and multivariate cox models were built to find covariates related to survival. Survival curves were calculated with the Kaplan–Meier method and differences between curves were determined using the log-rank test.

Results

Patient and tumor characteristics

The study cohort consisted of 200 tumors corresponding to 166 (83%) pheochromocytomas, 28 (14%) paragangliomas, and 6 (3%) metastases, collected from 190 patients (115 women and 75 men) with a mean age at diagnosis of 42.53 years (range, 7–82 years). Twenty-three patients presented a metastatic disease at diagnosis or within the follow-up period (median of 7.7 years from the initial diagnosis) with an equal distribution between synchronous and metachronous metastases. The proportion of patients with metastatic disease was consistent with their genetic status: 52% were metastatic in the group at high risk of progression (12/23 *SDHx*/*FH*/*SLC25A11*-mutated, cluster C1A) and 6.6% in other molecular groups (11/167 non-*SDHx*/*FH*/*SLC25A11*-mutated, clusters C1B, C2A/B/C). Twenty-seven samples from metastatic patients correspond to 21 primary tumors and 6 metastases. Using genomic data previously generated for this cohort (29), we first searched which tumors achieved immortalization.

Telomerase activation is prevalent in *SDHx*-metastatic PPGLs

To identify telomerase (+) tumors we analyzed expression levels of *TERT* using transcriptome data (11). General expression levels of *TERT* were very low in all PPGLs. Anyhow, we found a significant increase in *TERT* in transcriptomic cluster C1A enriched in tumors at high risk of metastatic progression (*SDHx*/*FH*-mutated), compared with other clusters (Supplementary Fig. S3A). Importantly, *SDHx* metastatic cases display the highest *TERT* expression even when compared with nonmetastatic tumors with the same genotype (Supplementary Fig. S3B). Given that full-length *TERT* can be co-expressed with a splice variant lacking the catalytic domain, the so-called β-deletion (35), we performed absolute quantifications of these variants using RT-qPCR. This validation revealed equivalent abundance of both full-length and β-deletion transcripts ($\geq 1.5 \times 10^{-4}$ copies) in 9 of 14

metastatic tumors from the high-risk group (Fig. 1A) and in 3 of 10 metastatic tumors from the other molecular groups (Supplementary Fig. S3C).

There are 3 major genetic/epigenetic alterations that can lead to transcriptional activation of *TERT* in tumors: enhancing promoter mutations (15), hypermethylation of the promoter region that includes the so so-called THOR region (TERT hypermethylated Oncological Region; ref. 16), and amplification of the locus (17). To determine the mechanisms underlying telomerase activation, we sequenced the *TERT* promoter region in tumor DNAs of the 200 PPGLs. We found 1 *SDHC*-mutated benign tumor carrying a non-enhancing C228A mutation (15) and 6 *SDHx*-mutated metastatic tumors carrying an enhancing C228T mutation (Fig. 1B). Interestingly, analysis of 3 samples from 1 of the individuals revealed that the C228T mutation was not present in the primary tumor, whereas it appeared in 1 out of the 2 metachronous metastases. Further analysis of methylation levels at the *TERT* promoter region using methylome data (36) revealed hypermethylation in 5 *SDHB*-mutated metastatic cases, including the aforementioned metachronous metastases (Supplementary Fig. S4A). Hypermethylation was significantly correlated with expression of *TERT* (Fig. 1C) and covered CpG islands spanning 4 Kb, including the so-called THOR region (ref. 16; Supplementary Fig. S4B), a finding confirmed using pyrosequencing (Supplementary Fig. S4C). Next, by examining the SNP array data, we identified copy-number gains involving the *TERT* locus (5p15.33) in 2 *SDHB*-mutated metastatic tumors (Fig. 1D). Interestingly, these samples also exhibit hypermethylation at the THOR region and presented the highest expression levels of *TERT*. Finally, no chromosomal rearrangements within 100 kb nearby the *TERT*

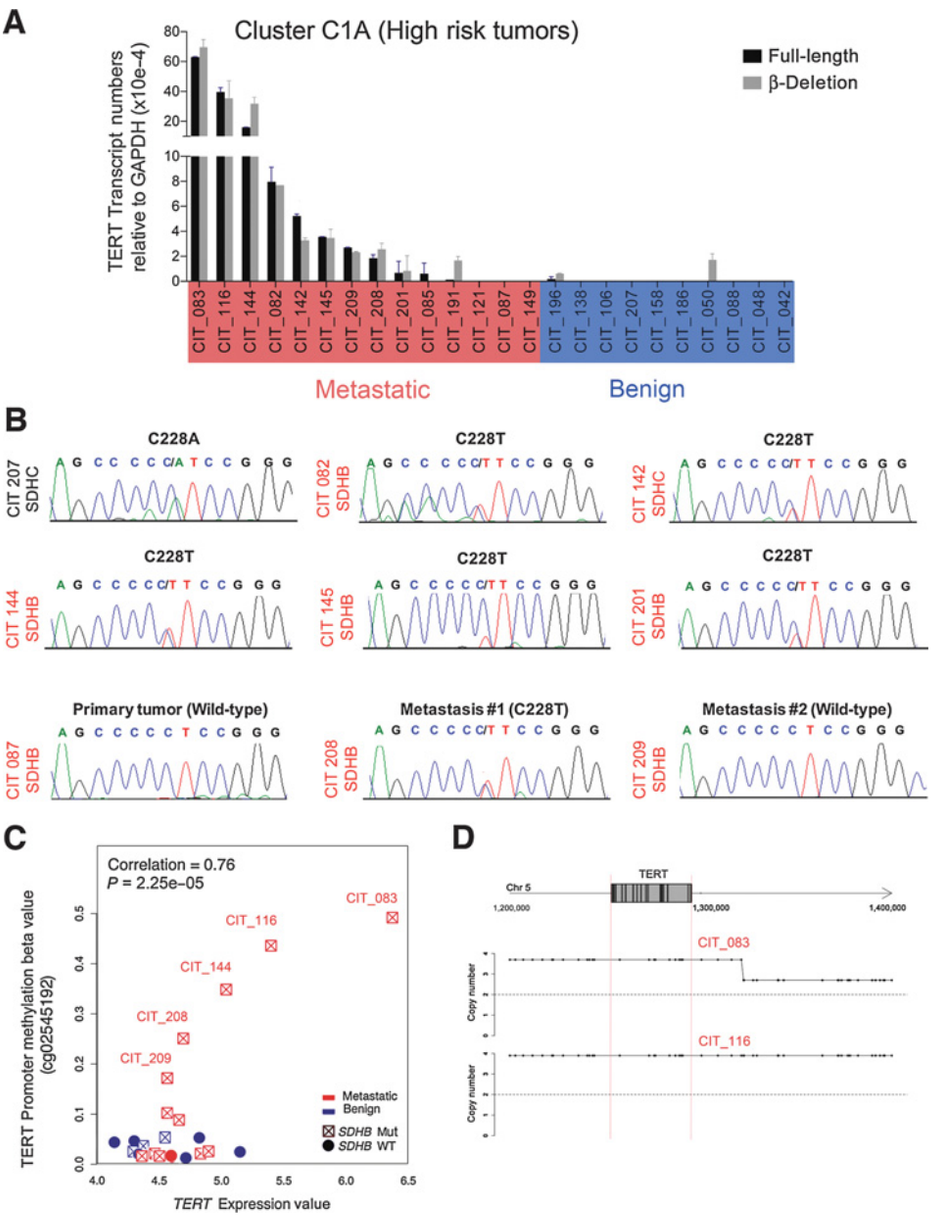

Figure 1.
Expression of *TERT* and underlying mechanisms. **A,** Expression levels of full-length *TERT* (black) and β-deletion splice variant (gray) in all tumors from the group at high risk of progression (*SDHx/FH*-mutated, cluster C1A). Absolute transcript copy numbers of *TERT* splice variants were normalized by transcript numbers of *GAPDH*. Mean ± SD from 2 independent RT reactions. **B,** Chromatograms corresponding to the identified *TERT* promoter mutations in *SDHx*-mutated patients. At the bottom, primary tumor and matched metastases from the same patient. Samples from patients with metastatic disease are in red print. **C,** Correlation analysis of *TERT* expression (Affymetrix data) and promoter methylation levels (Illumina 27 K, probe cg02545192) in the group of tumors at high risk of progression. The Pearson correlation coefficient and the correlation test *P* value are at the top left. **D,** Schematic representation of Chr 5 amplifications involving the *TERT* locus in 2 *SDHB*-mutated metastatic PPGLs.

locus were identified by whole-genome sequencing in the metastatic sporadic tumor CIT_015.

Taking into account a high co-expression of *TERT* splice variants, which was coupled to an underlying mechanism in most cases, we assigned a telomerase (+) status to 12 PPGLs, all of which were metastatic. Interestingly, 9 of 12 were tumors classified in the group at high risk of progression ($P = 2.42e{-}09$).

The ALT mechanism is activated irrespective of tumor subtype or metastatic status

ALT (+) tumors are characterized by displaying long and heterogeneous telomeres. We first estimated the telomere length of each tumor by applying slot blot analysis, and we focused on the 48 tumors exhibiting long telomeres, defined as those that fall above the third quartile (Fig. 2A). Next, samples for which material was available ($n = 22$ with long telomeres and $n = 7$ with intermediate/short telomeres used as controls) were assayed for telomere heterogeneity using APB assays (Fig. 2B; ref. 13). Twelve out of the 22 tumors with long telomeres were classified as ALT (+), whereas samples with intermediate/short telomeres were negative for the presence of APBs (Supplementary Table S2). We found that tumor samples with long telomeres harbor the lowest *ATRX* mRNA expression (Fig. 2C). Therefore, we used this criterion to assign the ALT (+) status to 9 additional tumors in which we could not perform APB assays.

Finally, we sought to determine the prevalence of *ATRX* mutations using a next-generation sequencing approach. In addition to the tumor carrying a frameshift mutation in *ATRX* that we have described previously (29), we identified 7 PPGLs, with damaging mutations (Table 1). Among them, expression of *ATRX* was absent at the protein level as confirmed by immunohistochemistry in available tissues (Supplementary Fig. S5). ALT characteristics were present in 6 of 8 (75%) tumors harboring *ATRX* mutations (Table 1), of which 2 had already been identified in the APBs screening, and 4 were thus considered as new ALT (+) cases.

Altogether, we assigned the ALT (+) status to 25 out of the 200 (12.5%) PPGLs of the cohort. In support of an ALT phenotype, we found that these tumors exhibit, as expected, higher levels of telomere repeat-containing RNA (*TERRA*) than telomerase (+) samples (Fig. 2D). Of note, although the ALT mechanism was activated irrespective of metastatic status or tumor subtype ($P = 0.169$), *ATRX* mutations were more frequent in tumors at high risk of metastatic progression ($P = 0.0014$).

Telomerase activation and *ATRX* mutations are independent prognostic factors

The exhaustive analysis of immortalization enabled us to determine that only 37 of 200 (18.5%) PPGLs activated a telomere maintenance mechanism (Fig. 3A), probably explaining why the great majority of these tumors never progress. Interestingly, telomerase activation appears to be more frequent in paraganglioma than in pheochromocytoma and the opposite was found for ALT (+) tumors (Fig. 3A). Furthermore, telomerase (+) but not ALT (+) tumors had a larger size than nonimmortalized tumors ($P < 0.05$; Fig. 3B).

It has been previously shown that tumor size (>5 cm), extra-adrenal location and *SDHB*-mutated status are clinical factors associated with metastatic progression and decreased overall survival (OS; ref. 9). Given that these variables appeared highly correlated with a telomerase (+) status, and given the tight association of *ATRX* mutations and the ALT phenotype in some metastatic tumors, we sought to identify which of these variables impact the most on the clinical outcome of affected patients.

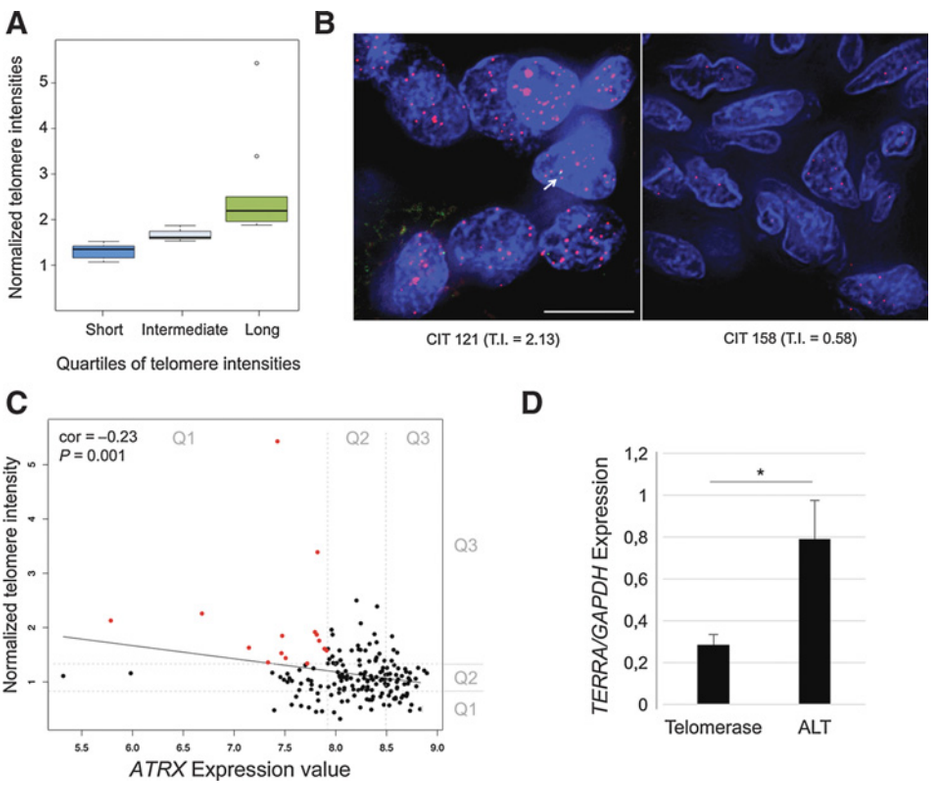

Figure 2.
Identification of ALT features in PPGLs. **A,** Box-plot shows normalized telomere intensities (measured by slot blot) discretized in 3 groups: Short, intermediate, and long, defined with the first, second, and third quartiles, respectively. **B,** Screening for the presence of large telomeric foci by telomeric FISH (red) and costaining with PML (green) for detection of ALT-APBs (arrow). Average projections of representative images with long and short telomeres are shown. T.I., telomere intensity. Each image is composed of 16 deconvolved stacks, 200 μm each; scale bar, 10 μm. **C,** Correlation analysis of *ATRX* mRNA expression level (Affymetrix data, $n = 187$) and telomere size for the entire PPGL cohort. The Pearson correlation coefficient and the correlation test *P* value are shown. The first and third quartiles are indicated as grey dotted lines. Red dots indicate tumor samples displaying both long telomeres and low *ATRX* mRNA expression. **D,** *TERRA* expression levels relative to *GAPDH* as determined by RT-qPCR are higher in ALT (+) than in telomerase (+) PPGLs (*, $P < 0.05$).

Table 1. *ATRX* mutations identified in the PPGL cohort

Sample ID	Driver PPGL mutation	*ATRX* cDNA mutation	Exon/Intron	Protein alteration	Consequence	Loss-of-function	Telomere intensity ± SEM	APB assay	ALT status
CIT_119	MET	6869A>G	Exon 32	Asn2290Ser	Missense	Yes	2.39 ± 0.74	Positive	ALT
CIT_191	SDHB	3967_3970del	Exon 12	Glu1323Glnfs*22	Frameshift	Yes	2.26 ± 0.10	N.A.	ALT
CIT_121	FH	5793del	Exon 25	Lys1936Argfs*19	Frameshift	Yes	2.13 ± 0.22	Positive	ALT
CIT_073		5114_5122del	Exon 19	Asn1705_Leu 1708delinsMet	In frame	N.D.	2.08 ± 0.08	N.A.	Probably ALT
CIT_078	VHL	7283A>G	Exon 35	Tyr2428Cys	Missense	Predicted	1.52 ± 0.14	N.A.	Probably ALT
CIT_149	SDHB	4778C>T	Exon 17	Ala1593Val	Missense	Predicted	1.39 ± 0.07	N.A.	Probably ALT
CIT_146		242+2T>A	Intron 4	p.?	Essential splicing	Yes	1.16 ± 0.29	N.A.	Probably WT
CIT_085	SDHB	1470_1548del	Exon 9	Gly491Leufs*45	Frameshift	Yes	1.11 ± 0.22	N.A.	Probably WT

NOTE: Next-generation sequencing identified 8/200 samples with *ATRX* mutations. Metastatic cases are highlighted in bold print. Positions of mutations with respect to their genomic location in cDNA, exon/intron positions and introduced changes at the protein level, as well as their functional consequences are specified. ALT (+) status was assigned on the basis of the presence of APBs or applying the combined criteria loss-of-function *ATRX* (predicted or determined by immunohistochemistry when possible) and long telomeres (telomere intensity ≥1.34).
Abbreviations: NA, not available material for analysis; ND, not determined; WT, Wild-type.

Univariate Cox regression models showed a strong impact of all of these covariates except tumor size and ALT phenotype, on both metastasis-free survival (MFS) and OS. Remarkably, multivariate analysis performed on the remaining covariates revealed that only telomerase activation and *ATRX* mutations were independent risk factors: MFS (hazard ratio, 48.2 and 33.1; $P = 6.50E{-}07$ and 1.90E−07, respectively); OS (hazard ratio, 33.1 and 12.9; $P = 2.60E{-}03$ and 2.20E−03, respectively; Table 2). In fact, 18 out of 27 tumor samples (67%) from the 23 patients with confirmed metastatic status harbor 1 of these alterations regardless the tumor subtype. Of note, these alterations were present not only in 7 primary tumors from patients with synchronous metastases, but also in 7 primary tumors from 6 patients with metachronous metastases (Supplementary Table S3). When combined, detection of telomerase activation and *ATRX* mutations reaches the best sensitivity (0.70) and specificity (0.99; Supplementary Table S4), thus performing more accurately (AUC 0.84) than the previously suggested risk factors on the ability to discriminate metastatic from nonmetastatic PPGLs.

To examine further the relationship between these alterations and prognosis, we performed survival analyses of the entire cohort. We found that patients with *ATRX*-mutated or telomerase (+) tumors exhibited a significantly shorter MFS and OS than patients without such alterations (log-rank tests $P < 0.001$; Fig. 3C and D). Similar results were obtained after excluding 6 metastatic samples from the analysis, of which 4 harbored these alterations (Supplementary Fig. S6). No statistically significant differences in MFS and OS between telomerase (+) and *ATRX*-mutated PPGLs were identified.

Strikingly, although the presence of telomerase activation and *ATRX* mutations greatly improved the stratification of patients at high risk of metastatic progression (*SDHx*/*FH*-mutated, cluster C1A; Fig. 4A–C), these alterations were present only in 5 out of the 13 (38.4%) metastatic tumors from the other molecular groups (clusters C1B, C2A/B/C; Fig. 4B and C). Therefore, we concluded that assessment of telomerase activation mechanisms and screening of *ATRX* mutations could be used to identify the metastatic potential of PPGLs, especially in tumors at high risk of progression.

Discussion

We here assigned a telomere maintenance mechanism to most tumor samples of the well-characterized cohort of 200 PPGLs collected by the COMETE network. We identified 12 telomerase (+) PPGLs, all of which having a metastatic status, and showed that both isoforms, full-length *TERT* and β-deletion, were overexpressed in these tumors. Although full-length is required for telomere maintenance, the catalytically dead β-deletion has also oncogenic functions (35, 37). Therefore, expression of both isoforms may promote cellular growth and progression to metastasis in PPGL tumors.

Mechanistically, hotspot mutations in the *TERT* promoter, C250T and C228T activate telomerase expression in human cancers (15) by creating a *de novo* binding motif for the transcription factor GABPA (38) and by driving an epigenetic switch (39, 40). We found 6 C228T hotspot promoter mutations exclusively in *SDHx*/*FH*-mutated metastatic tumors. This is consistent with previous studies, suggesting that although this mutation is not frequent in PPGLs, it can be found in *SDHx*-deficient tumors

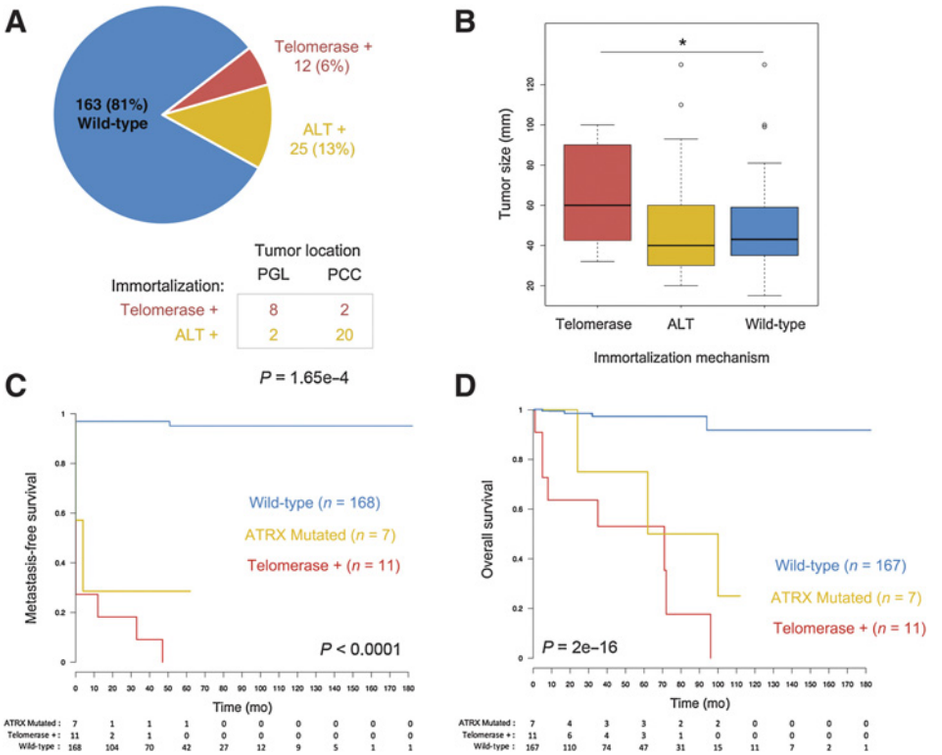

Figure 3.
Prevalence of immortalization mechanisms in PPGLs and association with clinical outcome. **A,** Distribution of telomere maintenance mechanisms among PPGL tumors (pie) and among tumor types (chart below). **B,** Box-plot of tumor size according to the immortalization status: telomerase (+), ALT (+), and nonimmortalized (wild-type) PPGLs (*, $P < 0.05$). **C,** MFS and (**D**) OS analyses of PPGLs for telomerase (+; red), *ATRX*-mutated (yellow) and wild-type tumors (blue) in the entire PPGL cohort. The log-rank test *P* values are shown.

(24, 25, 41). Our study is the first to show that this recurrent mutation is associated with overt metastatic disease.

Hypermethylation has been linked to *TERT* overexpression in numerous tumor types (16, 42), sometimes associated with worse prognosis (43, 44). A recent report also suggested this hypermethylation to be restricted to metastatic paraganglioma (26). Here, we reinforce this observation and highlight its relevance from the standpoint of diagnosis because even though *SDHx/FH*-mutated tumors display a hypermethylator phenotype (36), this is the first time that a specific alteration in methylation is associated directly with the metastatic status. In addition, we observed that hypermethylation is not mutually exclusive with *TERT* promoter mutations and copy-number gains. In fact, it has been shown that genomic rearrangements involving the *TERT* locus also coexist with hypermethylation of the THOR region in high-risk neuroblastomas (45). These observations suggest that distinct genomic alterations cooperate in driving the transcriptional activation of *TERT* in PPGLs and that analysis of *TERT* promoter mutations and methylation could be useful in the clinical routine to identify metastatic PPGLs in high-risk tumors.

Regarding the ALT immortalization mechanism, discrepant prevalences of 4% PPGLs (27) and 27% PPGLs (28) were reported based only histological data. To clarify this issue, we used a combined analysis of APB assays and low expression of *ATRX* in tumors with long telomeres, which enabled us to estimate that

Table 2. Univariate and multivariate cox analyses for MFS and OS

	Univariate analysis (MFS)				Multivariate analysis (MFS)		
	n	**Event (*n*)**	**HR (95% CI)**	***P***	***n***	**HR (95% CI)**	***P***
Tumor size	152	18	0.455 (0.18–1.2)	0.1			
Tumor location	183	20	9.76 (4–24)	4.20E−07	183	1.2 (0.34–4.2)	0.78
SDHB mutation	186	23	13.1 (5.7–30)	1.20E−09	183	1.51 (0.51–4.5)	0.45
Telomerase (+)	186	23	28.9 (12–68)	1.00E−14	183	48.2 (10–220)	**6.50E−07**
ALT (+)	182	20	3.38 (1.3–8.8)	0.013			
ATRX mutation	186	23	10 (3.7–27)	6.20E−06	183	33.1 (8.9–120)	**1.90E−07**

	Univariate analysis (OS)				Multivariate analysis (OS)		
	n	**Event (*n*)**	**HR (95% CI)**	***P***	***n***	**HR (95% CI)**	***P***
Tumor size	151	8	0.413 (0.09–1.7)	0.230			
Tumor location	182	11	11.9 (3.4–42)	1.00E−04	182	1.34 (0.09–19)	0.83
SDHB mutation	185	11	11.3 (3.4–37)	7.00E−05	182	1.06 (0.26–3.4)	0.93
Telomerase (+)	185	11	39.3 (10–150)	1.10E−07	182	97.4 (4.2–2,300)	**4.30E−03**
ALT (+)	181	9	0.63 (0.07–5.1)	0.670			
ATRX mutation	185	11	6.68 (1.7–26)	6.50E−03	182	44.1 (4–490)	**2.00E−03**

NOTE: Independent risk factors are highlighted in bold.
Abbreviations: CI, confidence interval; HR, hazard ratio; *n*, number of analyzed individuals.

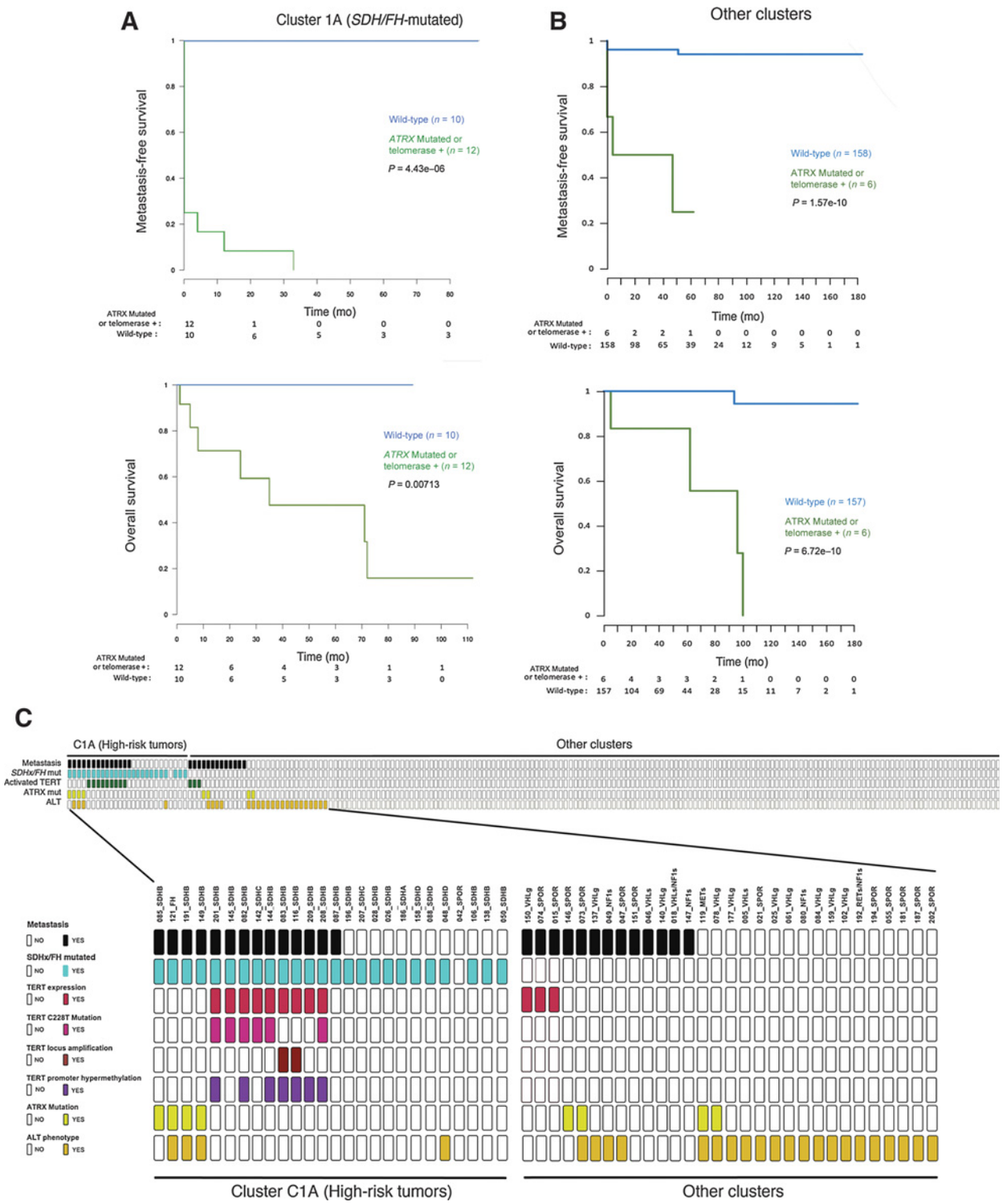

Figure 4.

Telomerase activation and *ATRX* mutations improve the stratification of high-risk *SDHB*/*FH*-mutated PPGLs. **A,** MFS and OS analyses of patients with PPGLs with telomerase (+) or *ATRX*-mutated tumors (green) compared with wild-type tumors (blue) from the high-risk group (cluster C1A) or from the other clusters (**B**). The log-rank test *P* values are shown. **C,** Summary of the genomic alterations linked to *TERT* overexpression, *ATRX* mutations, and ALT status found in the analyzed PPGL cohort. The metastatic status (black) and the PPGL driver mutation of each tumor are given at the top.

25 of 200 (12.5%) tumors, the great majority benign pheochromocytomas, activated the ALT mechanism.

We also find *ATRX* mutations in 8 of 200 PPGLs (4%), which contrasts with the original estimated prevalence of 12.6% (28). Accordingly, when exome-sequencing studies for PPGLs were revisited (Supplementary Table S5), the prevalence for *ATRX* mutations is 29 of 593 (4.8%). Of these, half have been associated with clinically aggressive behavior mostly in *SDHx*-mutated cases. Given that *ATRX* mutations are more frequent in this tumor subtype, this might explain why cohorts enriched for *SDHx* patients present a higher prevalence of *ATRX* mutations (28). We further found that only 6 of 25 (24%) ALT (+) PPGLs were linked to *ATRX* mutations and that these mutations had a stronger impact on poor prognosis than the ALT (+) status alone, particularly in PPGLs at high risk of metastatic progression (*SDHx*/*FH*-mutated, cluster C1A).

Our findings highlight a prominent role of immortalization-related mechanisms for the progression of neural-crest derived tumors, as noticed recently in neuroblastomas in which telomerase activation, *ATRX* mutations and *MYCN* amplifications define 3 nonoverlapping high-risk subgroups (46), or in gliomas in which mutations in the isocitrate dehydrogenase (*IDH*) and *TERT*/*ATRX* are also concurrent events that guide molecular classification and diagnosis (47).

Importantly, we could not assign any immortalization mechanism to 8 metastatic tumors, 6 of which from molecular groups C1B, C2A/B/C (Fig. 4C). This observation supports recent reports indicating that a subset of metastatic tumors, including melanomas and neuroblastomas could have progressed towards metastasis without activating a telomere maintenance mechanism (48, 49). On the contrary, our most striking result is that telomerase activation and *ATRX* mutations do impact the prognosis, particularly in the group at high risk of progression (cluster C1A). In fact, these alterations were present not only in metastatic samples and primary tumors from patients with synchronous metastases, but also in primary tumors long before the first metastasis appeared.

Interestingly, we found 1 patient with an *SDHB* mutation who developed 2 telomerase (+) metastases, even though his primary tumor operated on 7 years earlier was telomerase-negative (CIT_087). In addition, 1 patient presented with 2 primary tumors (CIT_073 and CIT_074), harboring an *ATRX* mutation and telomerase overexpression, respectively, 4 years before the first metastasis appeared. Thus, our results point these somatic alterations as key drivers of metastatic PPGLs. Nevertheless, we acknowledge caution with regard to the extent of heterogeneity within primary tumors of metastatic cases without evidence of telomerase activation or *ATRX* mutations. Given that extensive analyses of the whole tumor is impractical in the clinical routine, detection of these alterations in liquid biopsies would be of utmost importance to capture this tumor heterogeneity.

A key question in PPGL research is the identification of biomarkers able to distinguish between potentially metastatic and nonmetastatic tumors, which is crucial for diagnosis, treatment and follow-up. Although the present study is limited to the retrospective analysis of a modest sample of metastatic cases per molecular groups, our findings suggest that assessment of telomerase activation mechanisms (*TERT* promoter mutation/hypermethylation/copy-number gain or chromosomal rearrangement) and screening of *ATRX* mutations can identify potentially metastatic PPGLs, particularly in tumors carrying *SDHx*/*FH* mutations that are currently considered at high risk of progression. In addition, discrimination of immortalization mechanisms may become relevant to identify patients that would benefit from therapies targeting either telomerase or ALT (50). Prospective large multicenter studies will be required to address these issues, and to ascertain whether patients with *SDHx*-/*FH*–mutated PPGLs but without *TERT* activation or *ATRX* mutations would be henceforth considered as "low-risk" hereditary PPGLs for their surveillance.

Disclosure of Potential Conflicts of Interest

No potential conflicts of interest were disclosed.

Authors' Contributions

Conception and design: J. Favier, L.J. Castro-Vega, A.-P. Gimenez-Roqueplo
Development of methodology: I. Draskovic, L.J. Castro-Vega, A.-P. Gimenez-Roqueplo
Acquisition of data (provided animals, acquired and managed patients, provided facilities, etc.): I. Draskovic, A. Buffet, J. Cros, C. Lépine, T. Meatchi, M. Sibony, L. Amar, J. Bertherat, A. Londoño-Vallejo, J. Favier, L.J. Castro-Vega, A.-P. Gimenez-Roqueplo
Analysis and interpretation of data (e.g., statistical analysis, biostatistics, computational analysis): S. Job, I. Draskovic, N. Burnichon, A. Buffet, J. Cros, A. Venisse, V. Verkarre, A. de Reyniès, J. Favier, L.J. Castro-Vega
Writing, review, and/or revision of the manuscript: S. Job, I. Draskovic, N. Burnichon, J. Cros, L. Amar, J. Bertherat, A. de Reyniès, A. Londoño-Vallejo, J. Favier, L.J. Castro-Vega, A.-P. Gimenez-Roqueplo
Administrative, technical, or material support (i.e., reporting or organizing data, constructing databases): C. Lépine, A. Venisse, E. Robidel, J. Favier, A.-P. Gimenez-Roqueplo
Study supervision: J. Favier, L.J. Castro-Vega, A.-P. Gimenez-Roqueplo

Acknowledgments

A.-P. Gimenez-Roqueplo was supported by European Commission grants FP7 Research and Innovation funding program for 2007-2013 (n° 259735) and Horizon 2020 (n° 633983), and from Institut National du Cancer and Direction Générale de l'Offre de Soins (DGOS), Programme de Recherche Translationnelle en cancérologie (PRT-K 2014, COMETE-TACTIC, INCa_DGOS_8663). J. Favier received funding from Agence Nationale de la Recherche (ANR-2011-JCJC-00701 MODEOMAPP) and the Alliance nationale pour les sciences de la vie et de la santé (AVIESAN), Plan Cancer: Appel à projets Epigénétique et Cancer 2013 (EPIG201303 METABEPIC). N. Burnichon is funded by the Cancer Research for Personalized Medicine—CARPEM project (Site de Recherche Intégré sur le Cancer—SIRIC). The group is supported by the Ligue Nationale contre le Cancer (Equipe Labellisée). This work is part of the "Cartes d'Identité des Tumeurs (CIT) program" funded and developed by the Ligue Nationale contre le Cancer. Work in the Telomere and Cancer lab is supported by grants from La Ligue Nationale contre le Cancer (Equipe Labellisée) and Fondation ARC pour la recherche sur le cancer. We thank Profs Pierre-François Plouin and Xavier Bertagna for making this work possible through the COMETE Network, and to all members of the Genetics Department, Biological Resources Center and Tumor Bank Platform, Hôpital européen Georges Pompidou (BB-0033-00063), and of the Nikon Imaging Centre @ Institut Curie-CNRS (ANR-10-INSB-04) for technical support. We also thank Dr. Pedro Castelo-Branco and Dr. Joana Apolónio for providing technical assistance with pyrosequencing assay of the THOR region.

The costs of publication of this article were defrayed in part by the payment of page charges. This article must therefore be hereby marked *advertisement* in accordance with 18 U.S.C. Section 1734 solely to indicate this fact.

Received March 6, 2018; revised July 30, 2018; accepted October 3, 2018; published first October 9, 2018.

References

1. Lenders JW, Duh QY, Eisenhofer G, Gimenez-Roqueplo AP, Grebe SK, Murad MH, et al. Pheochromocytoma and paraganglioma: an endocrine society clinical practice guideline. J Clin Endocrinol Metab 2014;99: 1915–42.
2. Lloyd RV, Osamura RY, Kloppel G, Rosai J. WHO classification of tumours: pathology and genetics of tumours of endocrine organs. Lyon: IARC; 2017.
3. Buffet A, Morin A, Castro-Vega LJ, Habarou F, Lussey-Lepoutre C, Letouze E, et al. Germline mutations in the mitochondrial 2-oxoglutarate/malate carrier SLC25A11 gene confer a predisposition to metastatic paragangliomas. Cancer Res 2018;78:1914–22.
4. Favier J, Amar L, Gimenez-Roqueplo A. Paraganglioma and phaeochromocytoma: from genetics to personalized medicine. Nat Rev Endocrinol 2015;11:101–11.
5. Dahia PL. Pheochromocytoma and paraganglioma pathogenesis: learning from genetic heterogeneity. Nat Rev Cancer 2014;14:108–19.
6. Amar L, Bertherat J, Baudin E, Ajzenberg C, Bressac-de Paillerets B, Chabre O, et al. Genetic testing in pheochromocytoma or functional paraganglioma. J Clin Oncol 2005;23:8812–8.
7. Castro-Vega LJ, Buffet A, De Cubas AA, Cascon A, Menara M, Khalifa E, et al. Germline mutations in FH confer predisposition to malignant pheochromocytomas and paragangliomas. Hum Mol Genet 2014;23: 2440–6.
8. Amar L, Baudin E, Burnichon N, Peyrard S, Silvera S, Bertherat J, et al. Succinate dehydrogenase B gene mutations predict survival in patients with malignant pheochromocytomas or paragangliomas. J Clin Endocrinol Metab 2007;92:3822–8.
9. Ayala-Ramirez M, Feng L, Johnson MM, Ejaz S, Habra MA, Rich T, et al. Clinical risk factors for malignancy and overall survival in patients with pheochromocytomas and sympathetic paragangliomas: primary tumor size and primary tumor location as prognostic indicators. J Clin Endocrinol Metab 2011;96:717–25.
10. Castro-Vega LJ, Lepoutre-Lussey C, Gimenez-Roqueplo AP, Favier J. Rethinking pheochromocytomas and paragangliomas from a genomic perspective. Oncogene 2016;35:1080–9.
11. Burnichon N, Vescovo L, Amar L, Libe R, de Reynies A, Venisse A, et al. Integrative genomic analysis reveals somatic mutations in pheochromocytoma and paraganglioma. Hum Mol Genet 2011;20:3974–85.
12. Shay JW, Bacchetti S. A survey of telomerase activity in human cancer. Eur J Cancer 1997;33:787–91.
13. Dilley RL, Greenberg RA. ALTernative telomere maintenance and cancer. Trends Cancer 2015;1:145–56.
14. Borah S, Xi L, Zaug AJ, Powell NM, Dancik GM, Cohen SB, et al. Cancer. TERT promoter mutations and telomerase reactivation in urothelial cancer. Science 2015;347:1006–10.
15. Bell RJ, Rube HT, Xavier-Magalhaes A, Costa BM, Mancini A, Song JS, et al. Understanding TERT promoter mutations: a common path to immortality. Mol Cancer Res 2016;14:315–23.
16. Castelo-Branco P, Leao R, Lipman T, Campbell B, Lee D, Price A, et al. A cancer specific hypermethylation signature of the TERT promoter predicts biochemical relapse in prostate cancer: a retrospective cohort study. Oncotarget 2016;7:57726–36.
17. Zhang A, Zheng C, Hou M, Lindvall C, Wallin KL, Angstrom T, et al. Amplification of the telomerase reverse transcriptase (hTERT) gene in cervical carcinomas. Genes Chromosomes Cancer 2002;34:269–75.
18. Lovejoy CA, Li W, Reisenweber S, Thongthip S, Bruno J, de Lange T, et al. Loss of ATRX, genome instability, and an altered DNA damage response are hallmarks of the alternative lengthening of telomeres pathway. PLoS Genet 2012;8:e1002772.
19. Kinoshita H, Ogawa O, Mishina M, Oka H, Okumura K, Yamabe H, et al. Telomerase activity in adrenal cortical tumors and pheochromocytomas with reference to clinicopathologic features. Urol Res 1998; 26:29–32.
20. Kubota Y, Nakada T, Sasagawa I, Yanai H, Itoh K. Elevated levels of telomerase activity in malignant pheochromocytoma. Cancer 1998;82: 176–9.
21. Boltze C, Mundschenk J, Unger N, Schneider-Stock R, Peters B, Mawrin C, et al. Expression profile of the telomeric complex discriminates between benign and malignant pheochromocytoma. J Clin Endocrinol Metab 2003;88:4280–6.
22. Isobe K, Yashiro T, Omura S, Kaneko M, Kaneko S, Kamma H, et al. Expression of the human telomerase reverse transcriptase in pheochromocytoma and neuroblastoma tissues. Endocr J 2004;51: 47–52.
23. Luo Z, Li J, Qin Y, Ma Y, Liang X, Xian J, et al. Differential expression of human telomerase catalytic subunit mRNA by in situ hybridization in pheochromocytomas. Endocr Pathol 2006;17:387–98.
24. Liu T, Brown TC, Juhlin CC, Andreasson A, Wang N, Backdahl M, et al. The activating TERT promoter mutation C228T is recurrent in subsets of adrenal tumors. Endocr Relat Cancer 2014;21:427–34.
25. Papathomas TG, Oudijk L, Zwarthoff EC, Post E, Duijkers FA, van Noesel MM, et al. Telomerase reverse transcriptase promoter mutations in tumors originating from the adrenal gland and extra-adrenal paraganglia. Endocr Relat Cancer 2014;21:653–61.
26. Svahn F, Juhlin CC, Paulsson JO, Fotouhi O, Zedenius J, Larsson C, et al. Telomerase reverse transcriptase promoter hypermethylation is associated with metastatic disease in abdominal paraganglioma. Clin Endocrinol (Oxf) 2018;88:343–45.
27. Heaphy CM, Subhawong AP, Hong SM, Goggins MG, Montgomery EA, Gabrielson E, et al. Prevalence of the alternative lengthening of telomeres telomere maintenance mechanism in human cancer subtypes. Am J Pathol 2011;179:1608–15.
28. Fishbein L, Khare S, Wubbenhorst B, DeSloover D, D'Andrea K, Merrill S, et al. Whole-exome sequencing identifies somatic ATRX mutations in pheochromocytomas and paragangliomas. Nat Commun 2015;6:6140.
29. Castro-Vega LJ, Letouze E, Burnichon N, Buffet A, Disderot PH, Khalifa E, et al. Multi-omics analysis defines core genomic alterations in pheochromocytomas and paragangliomas. Nat Commun 2015; 6:6044.
30. Flynn A, Benn D, Clifton-Bligh R, Robinson B, Trainer AH, James P, et al. The genomic landscape of phaeochromocytoma. J Pathol 2015;236:78–89.
31. Juhlin CC, Stenman A, Haglund F, Clark VE, Brown TC, Baranoski J, et al. Whole-exome sequencing defines the mutational landscape of pheochromocytoma and identifies KMT2D as a recurrently mutated gene. Genes Chromosomes Cancer 2015;54:542–54.
32. Toledo RA, Qin Y, Cheng ZM, Gao Q, Iwata S, Silva GM, et al. Recurrent mutations of chromatin-remodeling genes and kinase receptors in pheochromocytomas and paragangliomas. Clin Cancer Res 2016;22: 2301–10.
33. Fishbein L, Leshchiner I, Walter V, Danilova L, Robertson AG, Johnson AR, et al. Comprehensive molecular characterization of pheochromocytoma and paraganglioma. Cancer Cell 2017;31:181–93.
34. Plouin PF, Gimenez-Roqueplo AP, Bertagna X. [COMETE, a network for the study and management of hypersecreting adrenal tumors]. Bull Acad Natl Med 2008;192:73–82.
35. Listerman I, Sun J, Gazzaniga FS, Lukas JL, Blackburn EH. The major reverse transcriptase-incompetent splice variant of the human telomerase protein inhibits telomerase activity but protects from apoptosis. Cancer Res 2013;73:2817–28.
36. Letouze E, Martinelli C, Loriot C, Burnichon N, Abermil N, Ottolenghi C, et al. SDH mutations establish a hypermethylator phenotype in paraganglioma. Cancer cell 2013;23:739–52.
37. Hrdlickova R, Nehyba J, Bose HR Jr.Alternatively spliced telomerase reverse transcriptase variants lacking telomerase activity stimulate cell proliferation. Mol Cell Biol 2012;32:4283–96.
38. Bell RJ, Rube HT, Kreig A, Mancini A, Fouse SD, Nagarajan RP, et al. Cancer. The transcription factor GABP selectively binds and activates the mutant TERT promoter in cancer. Science 2015;348:1036–9.
39. Stern JL, Theodorescu D, Vogelstein B, Papadopoulos N, Cech TR. Mutation of the TERT promoter, switch to active chromatin, and monoallelic TERT expression in multiple cancers. Genes Dev 2015; 29:2219–24.
40. Akincilar SC, Khattar E, Boon PL, Unal B, Fullwood MJ, Tergaonkar V. Long-Range chromatin interactions drive mutant TERT promoter activation. Cancer Discov 2016;6:1276–91.
41. Vinagre J, Almeida A, Populo H, Batista R, Lyra J, Pinto V, et al. Frequency of TERT promoter mutations in human cancers. Nat Commun 2013;4:2185.

42. Barthel FP, Wei W, Tang M, Martinez-Ledesma E, Hu X, Amin SB, et al. Systematic analysis of telomere length and somatic alterations in 31 cancer types. Nat Genet 2017;49:349–57.
43. Castelo-Branco P, Choufani S, Mack S, Gallagher D, Zhang C, Lipman T, et al. Methylation of the TERT promoter and risk stratification of childhood brain tumours: an integrative genomic and molecular study. Lancet Oncol 2013;14:534–42.
44. Bougel S, Lhermitte B, Gallagher G, de Flaugergues JC, Janzer RC, Benhattar J. Methylation of the hTERT promoter: a novel cancer biomarker for leptomeningeal metastasis detection in cerebrospinal fluids. Clin Cancer Res 2013;19:2216–23.
45. Peifer M, Hertwig F, Roels F, Dreidax D, Gartlgruber M, Menon R, et al. Telomerase activation by genomic rearrangements in high-risk neuroblastoma. Nature 2015;526:700–4.
46. Valentijn LJ, Koster J, Zwijnenburg DA, Hasselt NE, van Sluis P, Volckmann R, et al. TERT rearrangements are frequent in neuroblastoma and identify aggressive tumors. Nature Genet 2015;47:1411–4.
47. Cancer Genome Atlas Research N, Brat DJ, Verhaak RG, Aldape KD, Yung WK, Salama SR, et al. Comprehensive, integrative genomic analysis of diffuse lower-grade gliomas. N Engl J Med 2015;372:2481–98.
48. Dagg RA, Pickett HA, Neumann AA, Napier CE, Henson JD, Teber ET, et al. Extensive proliferation of human cancer cells with ever-shorter telomeres. Cell Rep 2017;19:2544–56.
49. Viceconte N, Dheur MS, Majerova E, Pierreux CE, Baurain JF, van Baren N, et al. Highly aggressive metastatic melanoma cells unable to maintain telomere length. Cell Rep 2017;19:2529–43.
50. Reddel RR.Telomere maintenance mechanisms in cancer: clinical implications. Curr Pharm Des 2014;20:6361–74.